

# Prediction of crack path in concrete-like composite using extended finite element method

Jakub Gontarz<sup>1\*</sup> , Jerzy Podgórski<sup>1</sup> 

<sup>1</sup> Faculty of Civil Engineering and Architecture, Lublin University of Technology, Lublin, Poland

\* Corresponding author's e-mail: [j.gontarz@pollub.pl](mailto:j.gontarz@pollub.pl)

## ABSTRACT

This paper presents the results of computer simulations of a three-point bending test of a notched beam. The numerical model was built to resemble concrete, consisting of a matrix with mortar characteristics and aggregate grains contained in it. The simulation was performed using own method for predicting the direction of crack propagation, implemented in the Abaqus FEA system to cooperate with the XFEM (eXtended Finite Element Method) fracture simulation method. The direction of crack propagation is determined by the procedure based on the stresses at the integration points around the crack tip propagating during the test. The crack is guided in the direction of the greatest decrease in the maximum principal stresses around the crack tip. The goal of this work was to introduce improvements to the existing algorithm so that it could simulate a crack in a heterogeneous material such as concrete. Currently, the implemented algorithm works only for materials modeled as homogeneous. In the literature available to date, no attempts have been found to model crack propagation using the XFEM method in simulations with heterogeneous material. The expected result was that a crack heading towards the grain of the aggregate would surround the grain. To verify the effectiveness of the method, it was first verified on several models with one large aggregate grain or two grains occurring in the path of the predicted crack. The paper also contains a description of the simulation with actual grain distribution and the problems associated with such simulation. It turned out that in simulations with one or two grains the algorithm copes correctly - the crack bypasses the grain. With actual graining there are problems related to the too complicated stress field in the vicinity of the grains and the crack does not reach the end of the sample. The paper discusses several ways to solve this problem, which will be taken up in future publications.

**Keywords:** fracture mechanics, fracture criteria, Abaqus user subroutine, XFEM.

## INTRODUCTION

The authors of this paper so far created their own procedure for determining the direction of crack propagation in brittle materials. The developed method cooperates with the eXtended Finite Element Method in the Abaqus FEA system [1]. It was programmed in Fortran language as Abaqus User Subroutine. The Abaqus system is an advanced engineering software package used for strength analysis of machine and structure elements and for simulation of nonlinear problems of solid and fluid mechanics. It uses the finite element method (FEM) to solve complex engineering problems. Several methods can be used to

simulate crack propagation in the Abaqus system, the most popular of which is the XFEM method. The XFEM method in Abaqus allows for modeling cracks without the need to change the finite element mesh. It allows for simulation of crack propagation by modifying the shape function using the so-called enrichment function [2]. This method is versatile and can be applied to various materials, such as metals, composites and ceramics. The XFEM method has the significant advantage that it does not require mesh modification at each crack increase or the creation of models with a very dense mesh, as is the case with methods based on element removal or separation. The calculations using this method are relatively fast

because only the shape functions of those elements that are likely to crack are enriched.

For the purposes of this paper, a modification of the existing procedure was proposed to simulate crack propagation in a non-homogeneous material with modeled aggregate such as concrete. This paper also describes how the modified procedure handles exemplary simulations, including different variants of the model with one and two aggregate grains. The main goal of the modification was to achieve a situation in which the crack bypasses the aggregate grain. The purpose of this article was therefore not to examine real samples with comparison to computer analysis, but only to present a modification of a previously written procedure that, for materials modeled as homogeneous, gave results consistent with reality, as shown in the authors' previous publications [3–5].

The effectiveness of the modified procedure was carried out on the basis of various simulations of three-point bending of notched concrete beam. This test has been used for a long time, but it is still an important topic discussed in the literature. Up to now, various analyses are carried out on its basis [6, 7]. Modeling of non-homogeneous materials for computer simulations is a common topic in the literature. In theory, the results of the model analysis at the meso-scale and at the macro-scale should be similar in terms of the crack path shape and load values. The issue of the influence of scale on the results of fracture simulation was discussed, among others, by Van Mier and Van Vliet [8].

Publications [9, 10] describe methods for modeling aggregate in the context of geometry in concrete samples for simulation purposes. Paper [11] presents a computational framework for modelling the fracture process in concrete. Other publications worth mentioning present the results of the fracture simulation of the aggregate model using FEM and DEM [12]. The results of [13] demonstrate the importance of modeling all aggregate classes to obtain an accurate description of the fracture behavior of concrete. Of course, concrete is not the only topic of the publication. There are descriptions of FEM analysis method of concrete from recycled aggregate [14], aluminum alloy sheet with grains [15] and polycrystals [16]. There are also publications starting to appear in the literature that explore the use of neural networks to aid in the analysis of fracture in concrete samples, such as [17–19], although in

this case it does not concern aggregate. Only a few publications deal with the fracture of inhomogeneous materials using the XFEM method. Paper [20] presents a modification of XFEM for testing concrete with fibers, [21] shows the XFEM implementation for simulation of fibre-reinforced polymers and [22] is about simulating frozen clay soils with grains using an XFEM-based computational homogenization. There is a lack of publications whose authors deal with the implementation of crack propagation criteria in composite materials similar to concrete. In the literature describing methods for predicting the path of crack propagation in heterogeneous materials, for example, the work of Sukumar and Srolovitz [23], which describes the fracture of a crystalline material. In it, the authors used an FEM mesh consistent with the structure of the material and the crack was modeled by disconnecting the mesh at the nodes without changing its geometry, which required a very dense mesh of elements. It did not use element partitioning, introducing mesh densification, or by using the XFEM method.

## METHOD OF PREDICTING THE CRACK PATH

The Abaqus system allows for the simulation of crack propagation using the XFEM method [1]. Several built-in criteria can be used to determine the initiation and direction of crack propagation, including MAXS (maximum nominal stress) or QUADS (quadratic nominal stress), but they are not suitable for analyzing brittle materials. The appropriate criterion is MAXPS. Only four-node elements CPS4, CPS4R, CPX4, CPX4R are allowed for simulation, where S denotes a model in a plane stress state, X – an axisymmetric model, R – a reduced element with one integration point, as opposed to an element with 4 integration points. The direction of crack propagation determined by this criterion is the direction of normal stresses at the integration points closest to the crack tip. Abaqus rotates the stress tensor to the principal stresses, and the angle of rotation of the tensor is also the angle at which the crack will be guided for a given load increment. The decision whether or not a crack should propagate depends on a simple condition [24]:

$$\mu = \frac{\sigma_1}{f_t} > 1 \quad (1)$$

where:  $\mu$  – material effort,  $\sigma_1$  – maximum principal stresses (tensile stresses),  $f_t$  – tensile strength of the material.

As proven in previous publications of the authors [3–5] this method has many disadvantages, hence the criterion proposed by the authors has been created. It has already been described in detail in previous publications, therefore only brief information will be presented here, allowing to understand this paper. The criterion for the minimum gradient of the effort field around the crack tip used here is described in previous author’s paper [25]. The algorithm for determining the direction of propagation is similar to Khan’s algorithm [26], which determines the direction of propagation based on the angle at which we find the shortest radius connecting the crack tip to the elastic region in an elastic-plastic material. For brittle materials, this criterion is inapplicable due to the lack of a plastic region. In the proposed criterion, we look for the angle at which the gradient of the strain field, calculated in the direction of this radius, has the greatest slope. For ductile materials, these criteria give identical results.

The own procedure was written in Fortran as one of the Abaqus User Subroutine, i.e. UDMGINI (User Damage Initiation), which allows defining own propagation direction and crack initiation criterion. The main assumption of own method is to read the material effort value at a certain distance from the crack tip. For example, along the black bold line in Figure 1a. The range of reading the value along this circumference is from  $-90^\circ$  to  $90^\circ$  relative to the propagation direction obtained in the previous load increment. This angle should not be greater, because stresses too close to the already formed crack are too distorted.

Figure 1b shows the integration points in the immediate vicinity of the discussed line. At these points, stresses are read, principal stresses

are determined, and material effort is calculated using material parameters according to formula (1). Additionally, material effort values are corrected as if they were located at one distance from the crack tip using linear interpolation. A graph of the dependence of material effort on the angle around the crack tip is shown in Figure 1c. The algorithm fits a fourth-degree polynomial to these points, the minimum of this graph is found, and the angle for this minimum is passed to the program further as the crack propagation angle. The minimum value of the graph around the crack tip can also be interpreted as the direction of the fastest drop in the material effort value from the crack tip, which is the same as the direction of the maximum material effort gradient. These calculations are performed for each load increment during the simulation. Each time, the coordinates of the crack tip and the stress field around it change.

The size of the area from which the integration points are collected affects how many integration points will be included in the calculations. More integration points mean that the approximation polynomial will be more accurately fitted, but this area cannot lie too far from the crack tip, because the stresses exactly at the crack tip are most important. It was therefore decided that the area of collecting integration points will be set in real time during the calculations, so that it includes between 40 and 50 integration points. The described method is close to the analytical solution of the so-called Griffith’s crack [27], as shown in Figure 2.

The specified criterion offers two major benefits compared to the standard approach: it considers stresses from a wider range of points, not just those nearest to the crack tip. Additionally, the propagation angle in this method is unaffected by shear stresses. The built-in method determines the propagation angle by rotating the stress tensor making it highly sensitive to shear stresses, which are significantly disturbed near the crack tip.

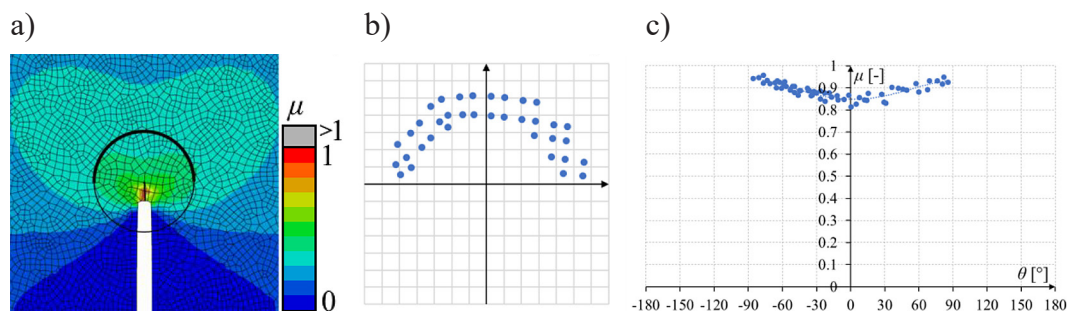


Figure 1. Method of determining the direction of crack propagation: (a) stress collecting area around the crack tip, (b) selected integration points, (c) material effort values in the considered area

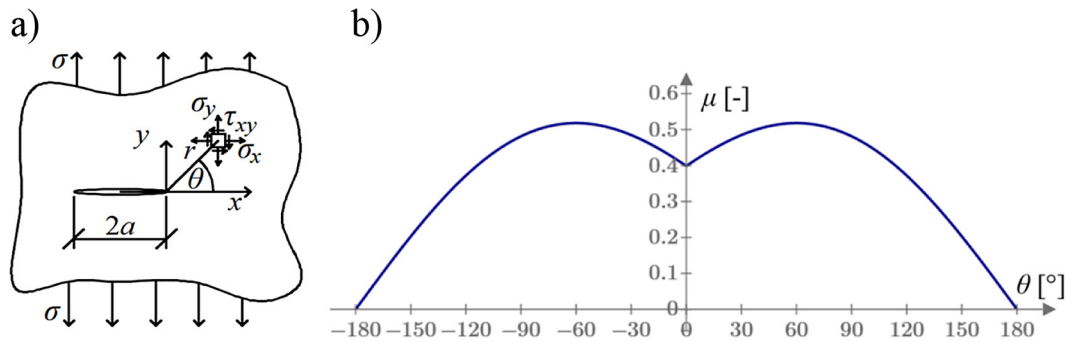


Figure 2. Griffith's crack: (a) scheme of the task, (b) values of material effort around the crack tip

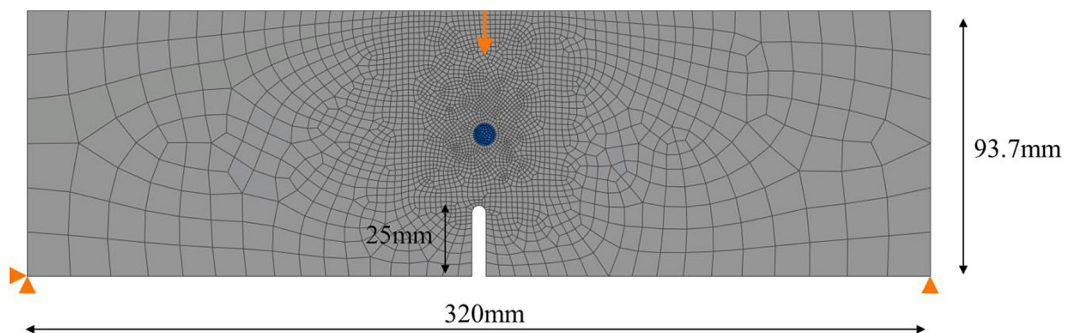


Figure 3. Simulation model

## COMPUTER SIMULATIONS

### Description of the model

Figure 3 presents the model used for the simulation, which was intended to verify the effectiveness of own procedure for determining the direction of crack propagation. This is a simple three-point bending test of a notched beam. The sample dimensions were taken from the authors' laboratory tests performed for earlier analyses, which are: 320 × 97.3 × 90.22 mm (width × height × depth) and with a notch length of 25 mm. The loading was controlled by a vertical displacement at the center of the top edge. The element type selected was CPS4. The finite element size varied from 0.5 mm to 15 mm. Initially, one 8 mm round aggregate grain was modeled approximately halfway up the predicted crack propagation line, with a slight offset to the right to force the crack to go around the aggregate grain on the left.

The goal of this research is to verify the effectiveness of own procedure for determining the direction of crack propagation in composite materials. Thus, material parameters do not reflect the actual parameters of mortar and aggregate. They were estimated and selected so that the Young's

modulus and tensile strength of the aggregate were greater than for concrete. The material parameters necessary for simulation are for cement mortar: tensile strength  $f_t = 3.11$  MPa, Young's modulus  $E = 13.724$  GPa, and for aggregate:  $f_t = 15$  MPa,  $E = 200$  GPa. Common parameters for both materials are Poisson's ratio  $\nu = 0.1482$  and critical strain energy release rate in mode I of fracture  $G_{I0} = 0.04794$  N/mm.

### Model with one grain

#### *The influence of aggregate grain on the crack direction*

In this chapter, the simulation results of the above model will be presented. The Abaqus/Standard module was used for calculations, the XFEM method was used to simulate the crack, and the above-described own method was used to determine the direction of crack propagation.

Below, the path of the crack formed during the simulation will be analyzed, divided into several significant stages. The phenomena and causes of the aggregate circling the crack will be described. Figure 4 shows a map of the maximum principal stresses at the initial stage of the crack, when the crack tip has not yet approached

the aggregate grain. The crack starts at the notch tip. Material effort depends linearly on the values of the maximum principal stresses (it depends on the tensile strength of the material). Figure 4b shows the relationship between material effort and the angle around the crack tip. It is assumed that angle  $0^\circ$  is the horizontal direction to the right and the angle increases clockwise and decreases counterclockwise. The angle of propagation of the crack, i.e. the angle for which the minimum of the approximation polynomial to the points on the graph was obtained, is about  $90^\circ$  and this is the vertical direction upwards, which is consistent with the predictions. This minimum in the upward direction from the crack tip is also clearly visible in the Figure 4a.

When the crack reaches the aggregate grain, a problem occurs. The aggregate material has a much higher Young's modulus than the cement slurry, which means that the aggregate will have much higher stresses for the same deformation. However, the aggregate also has a higher tensile

strength, which according to the formula (1) means that there will be lower material effort values. This can be seen clearly in the Figure 1. The direction of crack propagation is the same as the value of the minimum of the approximation function. The graph shows that due to low values of material effort in the aggregate, it is for an angle of about  $-60^\circ$ , i.e. toward the grain. In this case, in the simulation, the crack passed through the aggregate grain, instead of circling it. It was therefore decided to introduce a change in the algorithm. Integration points belonging to the aggregate grain are completely omitted during the polynomial fitting. In the programmed subroutine, this is done by omitting points with a much lower material effort value. As can be seen in the graph in the Figure 5b, after omitting these points, the approximation curve has a minimum for an angle of  $-120^\circ$ , which means that the crack will circle the aggregate from the left side.

Returning to the example presented at the beginning of this chapter, the Figure 6 shows a

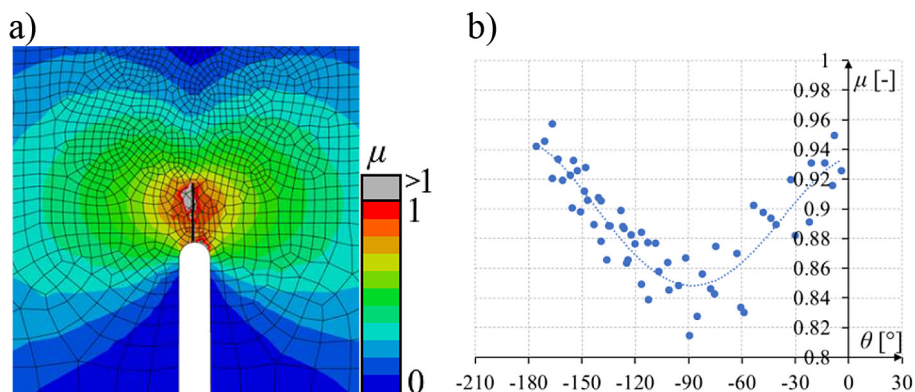


**Figure 4.** Initial stage of cracking of a model with one aggregate grain: (a) map of material effort values, (b) graph of the dependence of material effort on the angle around the crack tip

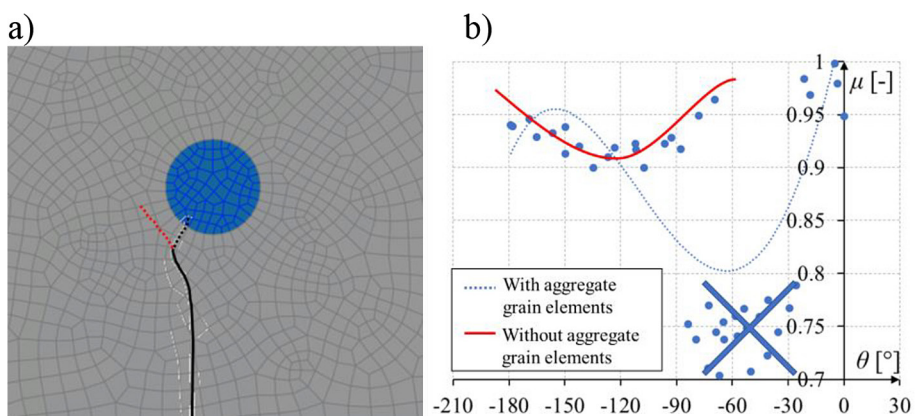


**Figure 5.** Example of determining the direction of crack propagation near the grain: (a) crack line, (b) graph of material effort

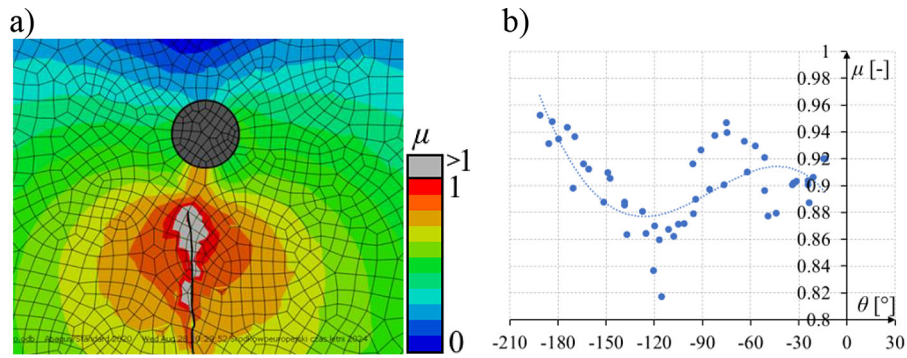


**Figure 6.** The stage where the crack approaches the aggregate grain: (a) map of material effort values, (b) graph of the dependence of material effort on the angle around the crack tip

further stage of crack propagation as it approaches the aggregate grain. After removing the points belonging to the aggregate (dark grey elements), it can be seen that the material effort in the cement slurry is greater near the grain, so that the polynomial minimum shifts to the left and the crack turns to the left.

In the subsequent stages shown in the Figure 7, a smooth change of the crack propagation angle circling the grain can be seen. In the Figure 7c, when the crack is already high above the grain,

the crack line is vertical, the stress field around the crack tip is similar to that at the very beginning of the simulation. The Figure 8 shows the last stage of the simulation when the crack approaches the edge of the sample. The integration point collection area around the crack tip largely goes outside the model, meaning that data for a large range of angles are missing (Figure 8b), but the procedure is still able to fit a polynomial to the existing points and thus find the minimum of the polynomial. The Figure 8c shows the complete crack path.

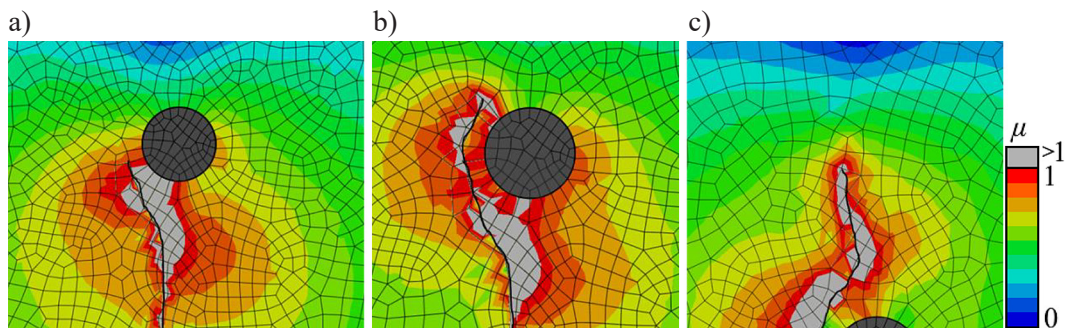


**Figure 7.** Next stages of crack propagation: (a) at the height of the grain, (b) above the grain, (c) much above the grain

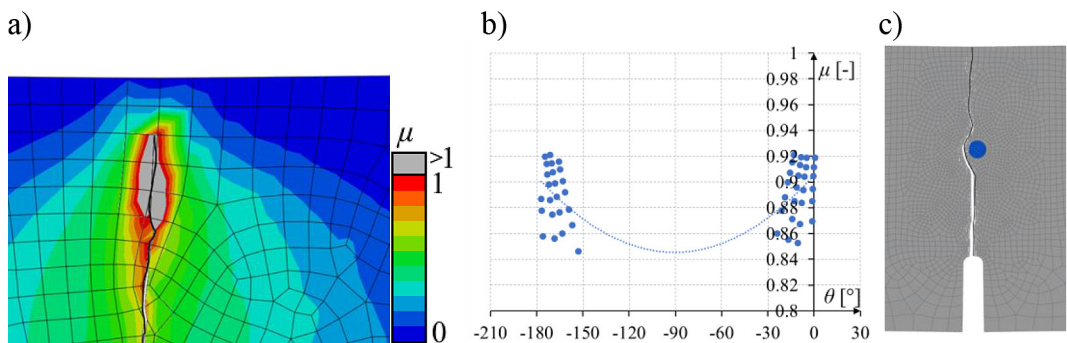


**Figure 8.** The final stage of simulation: (a) map of material effort values, (b) graph of the dependence of material effort on the angle around the crack tip, (c) full crack path

*Problem of crack branching*

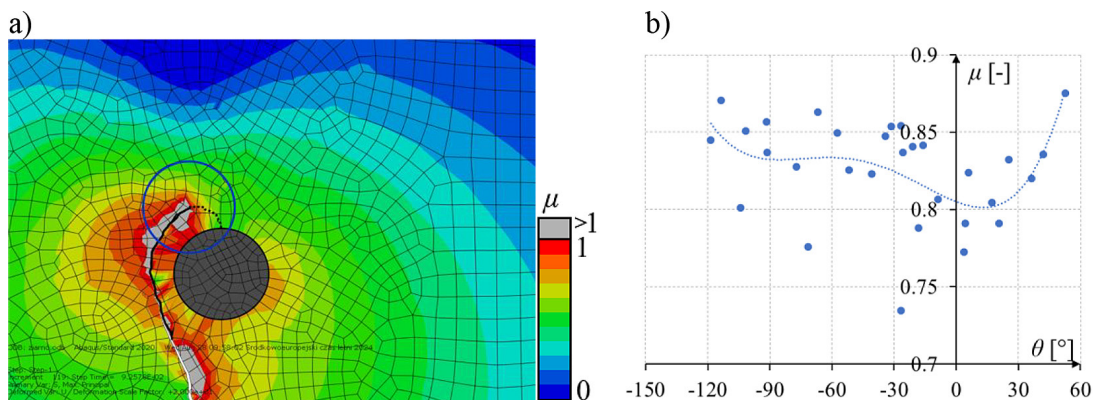
Work on the XFEM method has been ongoing for years. Unfortunately, the possibility of crack branching is still a problem that various authors have been trying to solve recently. There are proposals to implement the fracture branching support in the XFEM method [28, 29], but in the Abaqus system only one crack is available. The possibilities of subroutines application in Abaqus system are also limited. Subroutine UDMGINI requires to provide the condition of initiation and direction of propagation. If crack branching phenomenon were possible, developers would also have to redesign the way subroutines work. For this reason, the author’s method of predicting crack propagation direction does not allow for branching. In the case of the simple three-point bending problem of a notched beam, this phenomenon does not occur because the crack is directed symmetricaly vertically upwards. However, in the case of meso-scale simulations, where aggregate grains are present, the stress field is more complicated and the crack will branch, especially near the aggregate grains. This will also be the case in the presented simulation.

Figure 9a shows a map of the maximum principal stresses around the crack tip. Looking at the colours indicating the stresses, it can be seen that the location of the minimum stresses will change depending on the distance from the crack tip to the area of collecting integration points. For a small area around the crack tip, it is visible that the fastest decrease in the maximum principal stresses will be towards the right, downwards, i.e. towards the aggregate grain. For a large area, the minimum value of the principal

stresses is visible at the top of the figure and resembles a typical stress field without aggregate grain (see Figure 4). It can therefore be assumed that there are two views of the stress map around the crack tip - a more global one – when the crack goes vertically up, it depends on the model shape and loads, and a more local one, which is significantly influenced by the nearby grain. This causes the material stress graph to have two minima (Figure 9b), which would suggest crack branching. Since Abaqus cannot handle crack branching, the subroutine can only pass one crack propagation angle further to the calculation. For this reason, to unify the algorithm, it was decided to let the program code choose the smaller of the two minimum values. Moreover, it was also noticed that it is closer to the angle from the previous load increment.

Adjusting the size of the integration point area in the calculations allows controlling the crack. The direction Abaqus should choose in the case of branching can be determined. Increasing the integration point area moves closer to the global view, which can be seen in Figure 10.

In the case of a small number of integration points, the crack bends towards the aggregate grain and then the calculations are interrupted due to the inability to find a solution. For a larger area, the crack directs upwards to the upper edge of the model, bringing the simulation to an end. This means that in the case of crack branching, the more desirable result is the one obtained with a more global approach. Unfortunately, this gives rise to further problems, which will be described later. For further calculations, it was decided to choose 40 to 50 integration points around the crack tip at each load increment.



**Figure 9.** The problem of crack branching with 20–30 integration points: (a) map of material effort values, (b) graph of material effort values around the crack tip

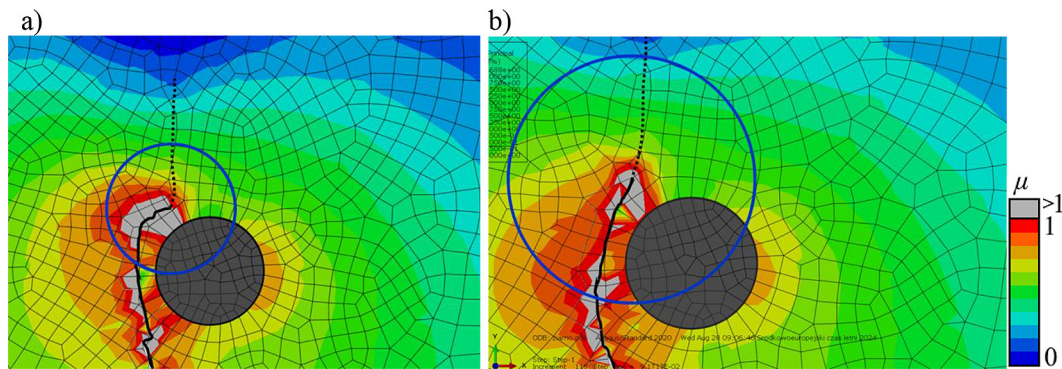


**Figure 10.** Calculated crack path around the grain: (a) 30–40 integration points included, (b) 40–50 integration points included

### Problem of material parameters

One of the most important problems that arise during the simulation are the material parameters of the cement slurry and aggregate, and in particular the ratio between the Young’s moduli of these two materials. In addition to the already assumed Young’s modulus of 200 GPa, it was also decided to perform the above simulation with the assumed Young’s modulus for the aggregate of 40 GPa, which is three times the Young’s modulus of the cement mortar.

Figure 11 shows the predicted fracture direction for two given values of the aggregate’s Young’s modulus. A higher Young’s modulus of the aggregate causes less grain deformation, which means that the same loads will cause greater stresses in the mortar near the grain. This causes the material effort values in the vicinity of the grain to be higher, which causes the minimum of the approximation curve to shift to the left, causing the crack to turn to the left. (see Figure 6). Less stress around the aggregate grain means the crack won’t turn to the left as much. It won’t

be “pushed” away from the grain. Therefore, in the case of a small aggregate Young’s modulus, the crack will turn towards the grain, which may be a desirable result in laboratory tests, especially for large grains, but the aim of this paper was to propose an algorithm that will lead to circling of the aggregate grain, therefore a high value of the aggregate Young’s modulus of 200 GPa was chosen for further simulations.

The explanation of this phenomenon can also be observed in the graph in Figure 11c. The material effort values at the integration points do not indicate this phenomenon, but the locations of the minimum of the approximation curves confirm this phenomenon.

### Other examples with one grain

Before proceeding to the full grain analysis, it was decided to run several more simulations to fully investigate all the mechanical phenomena occurring during the simulation and to ensure the effectiveness of the procedure. Figure 12 shows

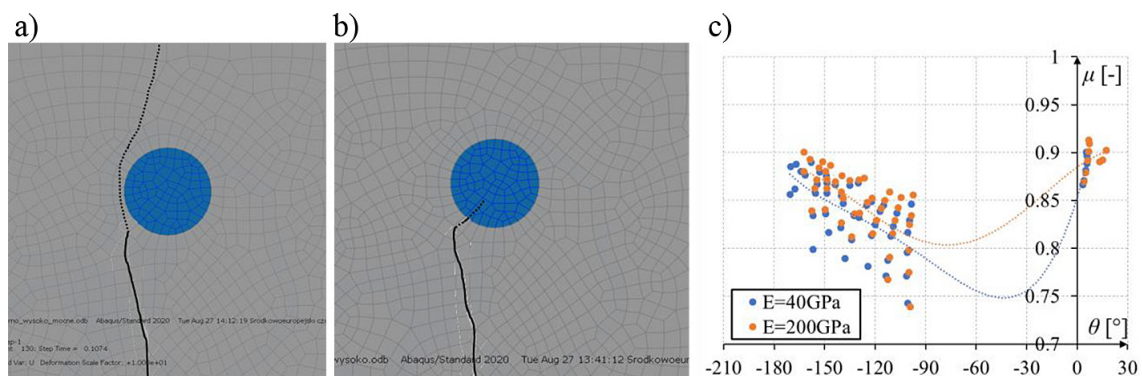


**Figure 11.** Problem of material parameters: a) crack path for  $E = 200$  GPa, b) crack path for  $E = 40$  GPa, c) graph of material effort values around the crack tip when the crack tip is below the grain

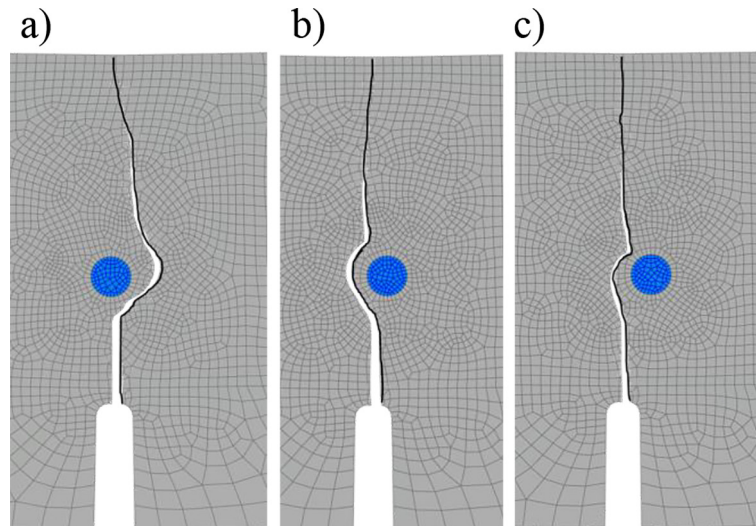


**Figure 12.** Crack simulations for different horizontal positions of aggregate grain: (a) grain in the middle, (b) grain shifted 2 mm to the right, (c) grain shifted 5 mm to the right

the results of the fracture simulation using own method for predicting the direction of crack propagation with different horizontal aggregate grain positions: grain in the center, shifted 2 mm to the right and shifted 5 mm to the right. All three simulations mainly differ in the position of the crack tip relative to the aggregate grain before it passes through. As it can be seen, no problems occurred here. For a grain positioned exactly in the middle, and therefore symmetrically, the choice of the propagation direction was certainly influenced by the finite element distribution. In actual laboratory test with such grain position, the crack should branch at the lower edge of the grain, but the grain should also stay on one side, causing the branch on only one side to continue propagating,

just like in simulation. The next step was to test the performance of the procedure with different vertical grain orientations and different grain sizes. These simulations prove that grain size influences the magnitude of stress around the grain in the mortar. Small grain (4 mm in simulations) is almost unnoticeable on the stress map. In the case of simulation with small grain (Figure 13a) it does not seem to significantly affect the crack line, therefore with small grain the procedure copes correctly. This is also in accordance with the literature [30, 31], where a significant effect of grain size on the shape of the cracked concrete sample is observed.

In the case of a large aggregate grain (16 mm in the simulation, Figure 13b), the problem of

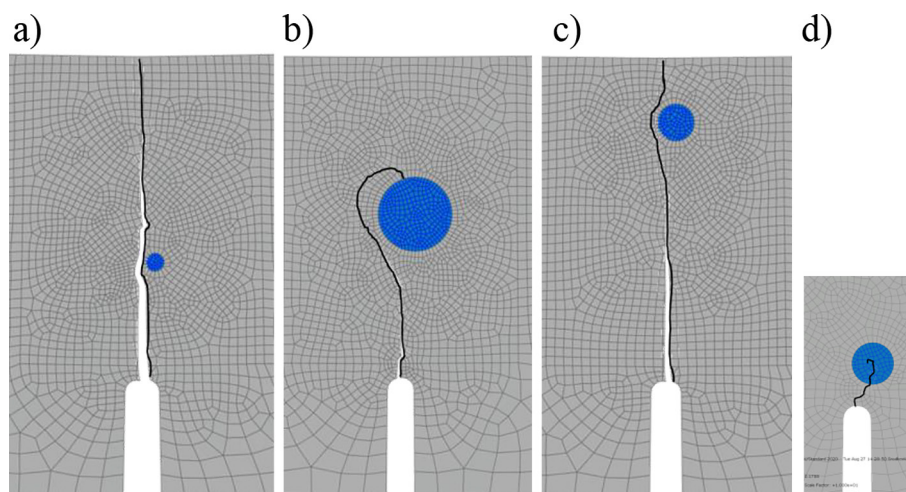


**Figure 13.** Crack simulations for couple different situations: (a) 4 mm grain, (b) 16 mm grain, (c) grain set high, (d) grain set low

crack branching, which was discussed earlier, returns. A large aggregate grain causes the stresses in the mortar near the grain to increase significantly, which means that the importance of the local minimum of the approximation curve increases. Increasing the size of the aggregate grain is therefore identical to reducing the area of collecting integration points around the crack tip. The solution to this problem could be to increase this area again. Unfortunately, this is not an ideal solution because the developed procedure was to be universal, and therefore should work for any aggregate size. By increasing the area of collecting integration points around the crack tip, the problem of crack branching can be solved for a large grain, but this also poses a risk that small grains will be unnoticed during calculations. In addition, in theory, the most important stresses are infinitely close to the crack tip, so further moving away from it will lead to increasingly incorrect results in a global perspective. For these reasons, it was decided to stick to the collection region of 40–50 integration points. In the future, it is planned to solve the problem of crack branching in a different way, which will be discussed in the summary.

Figure 13c shows the crack path for a grain positioned near the top edge of the model. In this case, no irregularities are observed. The fracture correctly reaches the top edge of the model, leading the simulation to completion. There occurs also a phenomenon shown in the Figure 8, when the integration point collection area goes beyond the model, but this does not prevent the procedure from finding the correct direction of crack propagation.

Figure 13d shows the fracture line for a low-set aggregate grain. Unfortunately, the fracture line is incorrect. The explanation for this phenomenon is given in Figure 14. Here, it can be seen that the highest drop in the maximum principal stresses is on the right side of the crack, instead of on the left. This is probably due to the close proximity of the notch, which means that the stresses around the crack tip cannot stabilize properly. Perhaps with different aggregate grain sizes or different horizontal positioning of the aggregate grain, this problem will not occur, but it was initially stated that a solution to this problem could be to refine the mesh near the top of the notch.

### Model with two grains

The above chapters describe the phenomena and behavior of the crack line using own method for predicting the direction of crack propagation with one aggregate grain. The main goal of the above analyses was to show that own procedure can circle the grain. The next analyses will be performed for two aggregate grains and will involve checking how the algorithm copes with a more complicated stress field. First, a model was analyzed in which there are two grains on the predicted crack path at a certain distance from each other, i.e. at different vertical levels, what is shown in Figure 15a. In this case, the simulation worked correctly because the grains had no significant influence on each other.

The next simulation is two grains next to each other, symmetrically positioned in the sample (Figure 15b). Due to symmetry, the crack is

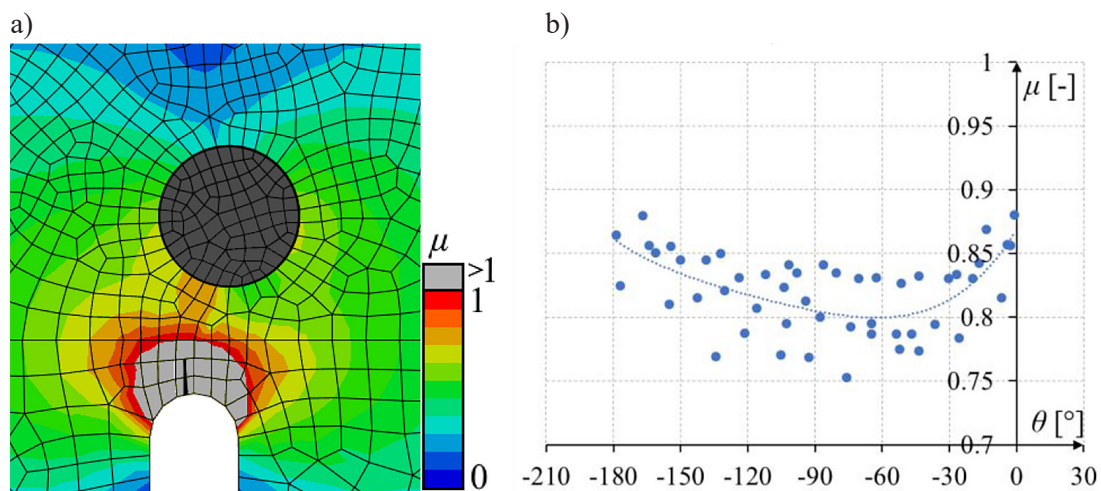
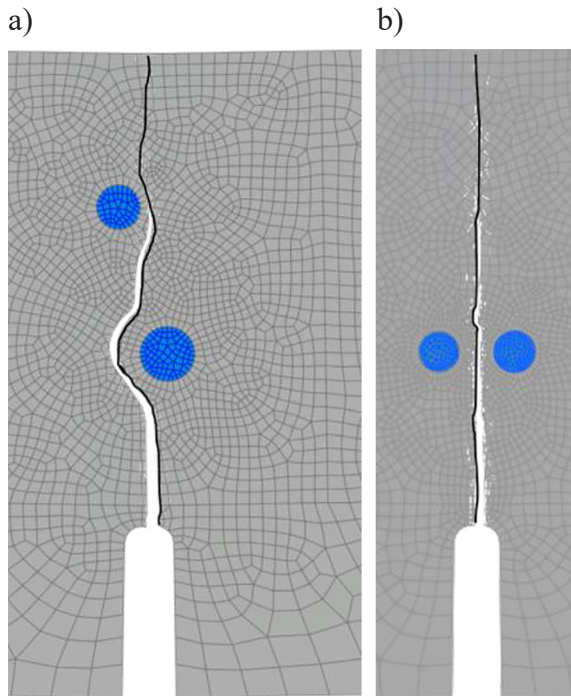


Figure 14. Explanation of the phenomenon occurring at low grain setting: (a) map of material effort values, (b) graph of material effort values around the crack tip



**Figure 15.** Crack paths for the model with two aggregate grains: (a) grains at different levels, (b) grains symmetrically next to each other

also expected to be symmetrical, i.e. vertical. However, an interesting phenomenon occurs here. The crack line passes correctly between the grains, but after bypassing them, a stress field appears similar to the one described in the explanation of crack branching. The stresses in the vertical upward direction increase, which causes the minimum of the approximation curve to shift to the left or right. The fracture line bends for a moment but stabilizes in the next load increments (Figure 15b).

An interesting phenomenon occurs when in the above simulation one grain is smaller than

the other. The stress field is not symmetrical. The maximum principal stresses are greater for larger grain (the effect of grain size on the stress magnitude in the cement slurry near grain has been discussed earlier). This means that the crack line will be “pushed” away from the larger grain (Figure 16). This movement of the crack away from the larger grain will be greater for a larger grain size ratio, for smaller distance between grains or for a larger Young’s modulus of the aggregate (increasing the Young’s modulus will significantly increase the stress around the larger grain and slightly increase the stress around the smaller grain). The dependence of the value of the aggregate Young’s modulus on the crack path is shown in Figure 17b-d. In contrast to Figure 11, in this case the more expected crack path is for a smaller Young’s modulus.

The solution to this problem seems to be to refine the finite element mesh, which would result in more elements between the grains. Simulations were performed for finite elements twice as small. In the case of a low Young’s modulus of the aggregate, the crack path is also correct (Figure 18a). In the case of a high Young’s modulus of the aggregate, the crack path correctly passes between the grains, instead of turning below them as previously for larger finite elements. Unfortunately, the problem of crack branching returns here (Figure 18b). For smaller finite elements, the integration point collection area around the crack tip also decreases. The ratio of grain size to the integration point collection area increases and the same situation as in the Figure 9a and Figure 13b appears. This means that the size of the finite elements has a strong influence on the crack line, or rather on the decision which path the program will choose when the crack branches.

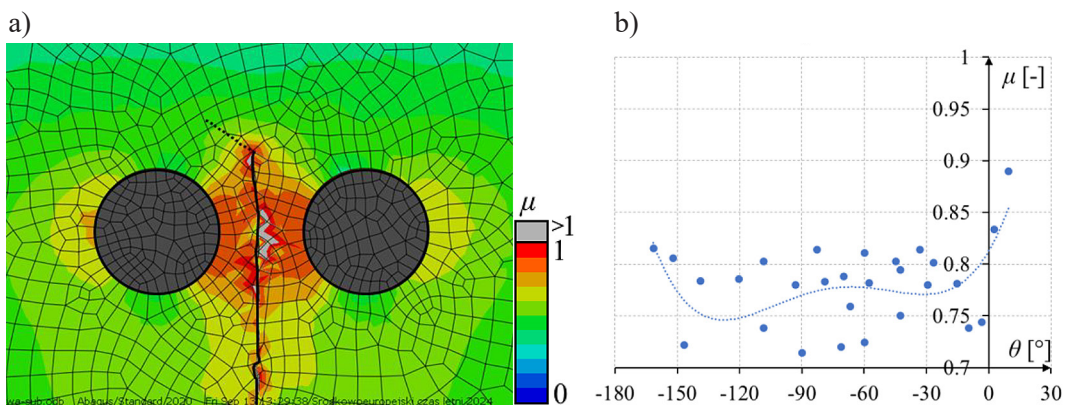


**Figure 16.** Explanation of the phenomenon occurring when two aggregate grains are placed next to each other: (a) map of material effort values, (b) graph of material effort values around the crack tip

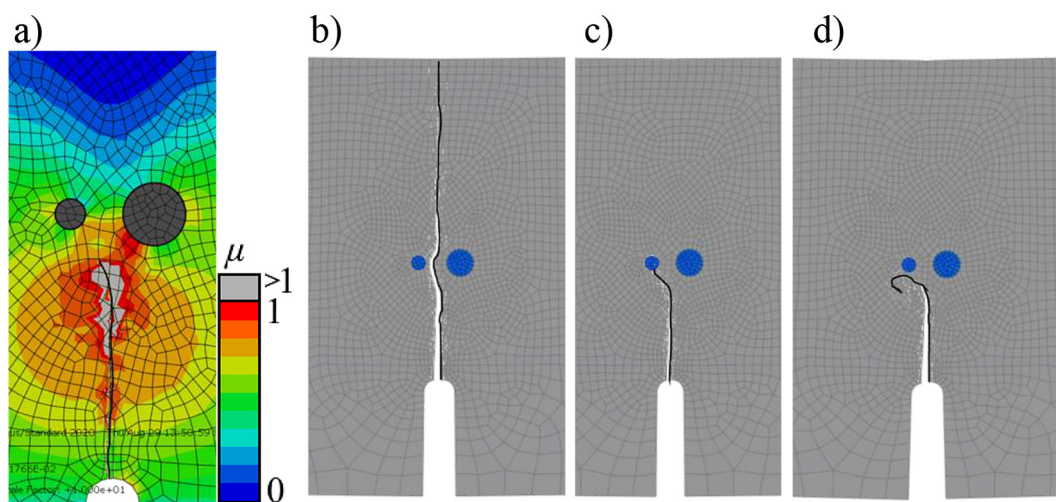


**Figure 17.** Simulations with two aggregate grains of different sizes: (a) map of material effort values, (b) crack path for aggregate with  $E = 40$  GPa, (c) crack path for aggregate with  $E = 100$  GPa, (d) crack path for aggregate with  $E = 200$  GPa

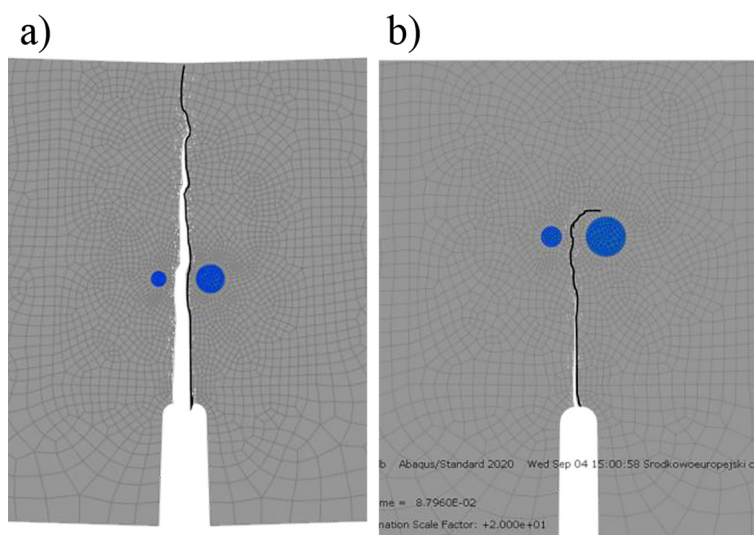


**Figure 18.** Simulations with two aggregate grains of different sizes for dense mesh: (a) crack path for aggregate with  $E = 40$  GPa, (b) crack path for aggregate with  $E = 200$  GPa

### Model with actual grain distribution

#### Random distribution generation

The last stage of the work is to conduct a simulation on a model with the actual grain distribution. In order to determine the correct distribution and proportions of aggregate grains in the concrete mix, the Fuller cumulative curve was used [32]. For the purposes of the discussed simulation, the authors wrote a Python script that generates random grain distribution in the Abaqus model. The script works as follows: the algorithm generates random coordinates and the diameter of the aggregate grain based on the user-specified limit values.

Then, it checks whether the newly generated grain does not overlap with any previously generated grain, also taking into account the user-specified minimum distance value. If it overlaps, the grain is rejected. The program repeats the algorithm until the percentage ratio of the grain surface to the total surface area of the model exceeds the user-specified value. Then, it creates the so-called “partition face”, i.e. the division of the part into sub-elements in Abaqus. Then, the aggregate material is manually assigned to the created circles.

The following parameters were set for the script:  $d_{\min} = 2$  mm – minimum grain diameter,  $d_{\max} = 10$  mm – maximum grain diameter,

minimum distance between grains = 1 mm, minimum grain to total area ratio = 0.2. It turned out that the distribution obtained using the programmed script (Figure 19b) is very similar to the one proposed by Fuller (Figure 19a). Variable on the graph are:  $d_0$  – diameter of the current grain,  $p_c(d < d_0)$  – number of grains with diameters smaller than  $d_0$ ,  $P_k$  – the number of all grains.

For the purpose of this simulation, the average finite element size was assumed to be 0.3 mm. A section of the model mesh is shown in Figure 20. In order to save computational time and computer power, the grain distribution in the area only on a small width along the predicted crack path was generated. The rest of the model is filled with homogenized material.

### Simulation results

The fracture simulations of the above proposed model with actual grain distribution were performed using own method for predicting the direction of crack propagation. Unfortunately, the simulation failed. The calculations were interrupted around the second or third passed grain, by the inability to find a finite element solution. The resulting crack path is unrealistic. The simulation was performed multiple times for different random grain distributions, without any apparent success. The Figure 21 shows examples of failed simulations. Attention should be paid to the very complex, almost chaotic stress field, which results from the many aggregate grains occurring

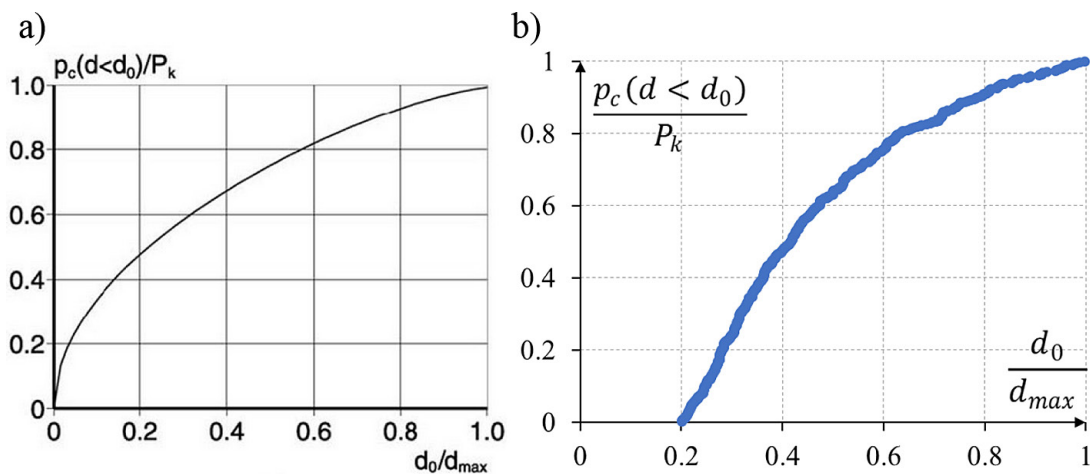


Figure 19. Aggregate grain distribution curve in concrete: (a) curve proposed by Fuller, (b) curve obtained for simulation purposes

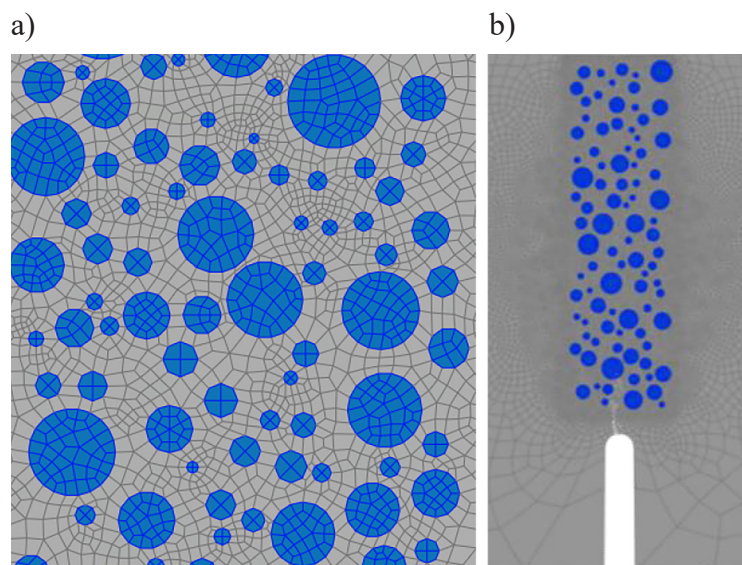


Figure 20. An actual grain distribution: (a) small section of the model, (b) wider view

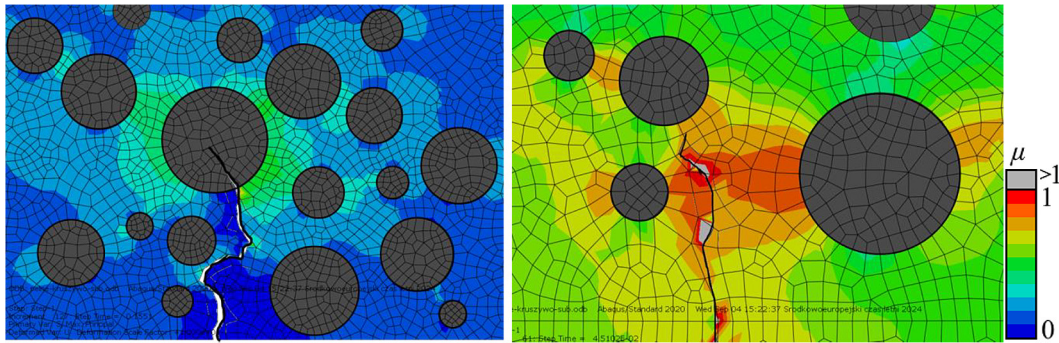


Figure 21. Examples of failed simulation results

nearby. The map of maximum principal stresses is too complicated to find the minimum of the graph of material effort approximation curve. Additionally, all the above-mentioned phenomena occur here, which made the above simulations difficult for one and two aggregate grains: the problem of crack branching, the problem related to the values of Young’s modulus of the aggregate, the problem of “repulsion” of the crack from the aggregate grain in the case of two different grains close to each other. The issue of selecting the size of the integration point collection area relative to the grain size near the crack tip is very important here.

Unfortunately, the solution to the problem cannot be the reduction of finite element size. In the case of such a large number of grains in the vicinity of the crack tip, the area of collecting integration points should not be moved far away, while too small an area will cause an even more pronounced phenomenon of selecting the wrong crack path in the case of branching.

Another very important problem related to reducing the size of finite elements is the computation time and insufficient computer resources. This problem is related to the limitations that the Abaqus system gives the user for programming subroutines. Reading stresses in the model is done by opening each increment the “results” text file with data at all integration points in all previous load increments. This file for large models can grow to several gigabytes, and the number of increments in the simulation range from hundreds to thousands.

Only a twofold reduction in the finite element size leads to a fourfold increase in the number of elements and a twofold increase in the number of load increments. This means that the result file will be 8 times larger. This file will be read twice as often, so it can be estimated that

the calculations will be 16 times longer. Unfortunately, time itself is not the only problem. At a certain stage, the computer is unable to save and read such large text files. Unfortunately, at the stage of writing the subroutine, the user has no influence on the results file, so it seems that the solution to this problem can only be to create own software, on which the programmer can have full control. For this reason, the next stage of work will be to find a way to determine the correct crack line in the model with the real grain distribution without increasing the number of finite elements. The own procedure, as proven in previous publications, copes very well with predicting crack propagation in macro-scale models with a very small number of finite elements.

## CONCLUSIONS

For the purpose of this paper, own procedure for predicting fracture propagation in Abaqus using XFEM to simulate the fracture was improved and tested. This improvement consisted in adapting the algorithm to simulate concrete-like materials with modeled aggregate. Several models with one and two aggregates were analyzed. The simulations performed mostly gave correct results of crack paths and allowed to describe many phenomena occurring during fracture of such materials.

Unfortunately, it turned out to be impossible to simulate the actual distribution of aggregate grains in the model due to the very chaotic stress field. One of the most important reasons is the problem related to the crack branching phenomenon, which the XFEM in Abaqus software does not allow. Branching is strongly related to mesh size or grain size, because the ratio between the grain size and the size of the area of collected integration points changes. The solution to the

problem of crack branching may be to force the crack to pass very close to the grain, so that the crack does not have the opportunity to turn towards the grain (see Figure 9). Unfortunately, the XFEM method does not allow for guiding the crack exactly between two finite elements but relies on dividing one element. Maybe it is possible to force the crack to pass as close as possible to the grain edge using an additional weaker layer between the mortar and the grain (ITZ layer) with a thickness of one finite element.

The material parameters are also a problem – the crack passes through the aggregate with a low Young's modulus, but it avoids the aggregate with a high Young's modulus.

In the next stage, a number of improvements to the discussed simulations are planned: modeling the ITZ layer between the aggregate and the concrete, as mentioned above, so that the area of collecting integration points can be reduced to a minimum. Another idea is to try to transform the programmed criterion so that it is not necessary to remove integration points in the aggregate (e.g. another way of finding the minimum of the material effort diagram). In the case of successful simulations after the introduction of the above plans, it is also worth considering: performing simulations with a grain shape other than circular, performing laboratory tests to precisely determine the material parameters (especially Young's modulus and tensile strength of aggregate and cement), performing laboratory tests of the analyzed simulations to compare the fracture lines, performing simulations using other methods for comparison (e.g. the Concrete Damage Plasticity method in the Abaqus system).

It is also possible that XFEM is completely not suitable for simulating the cracking of models with aggregate. Despite the unsuccessful simulation of models with modeled real aggregate distribution, it can be considered that the goal of the paper set at the beginning has been achieved. Own method of predicting the direction of crack propagation can cope with the model with aggregate grain, because the crack line goes around the grain. However, this is not the end of the work and it is necessary to implement further ideas.

### Acknowledgements

This research was supported by the Lublin University of Technology Science Financing Subsidy. FD-20/IL-4/019 and FD-20/IL-4/041.

### REFERENCES

1. Abaqus Documentation. <http://130.149.89.49:2080/v6.14/index.html>
2. Moës N., Dolbow J., Belytschko T. A finite element method for crack growth without remeshing. *International Journal for Numerical Methods in Engineering*, 1999, 46(1), 131–150. [https://doi.org/10.1002/\(SICI\)1097-0207\(19990910\)46:1<131::AID-NME726>3.0.CO;2-J](https://doi.org/10.1002/(SICI)1097-0207(19990910)46:1<131::AID-NME726>3.0.CO;2-J)
3. Gontarz J., Podgórski J. The computational method of predicting the crack path in confrontation with laboratory tests. *Advances in Science and Technology. Research Journal*, 2023, 17(2), 90–110. <https://doi.org/10.12913/22998624/161007>
4. Gontarz J., Podgórski J. Simulation of the Griffith's crack using own method of predicting the crack propagation. *Advances in Science and Technology. Research Journal*, 2021, 15(4). <https://doi.org/10.12913/22998624/141908>
5. Gontarz J., Podgórski J. Comparison of various criteria determining the direction of crack propagation using the UDMGINI user procedure implemented in Abaqus. *Materials*, 2021, 14(12). <https://doi.org/10.3390/MA14123382>
6. Balamuralikrishnan R., Al-Mawaali A. S. H., Al-Yaarubi M. Y. Y. et al. Seismic upgradation of rc beams strengthened with externally bonded spent catalyst based ferrocement laminates. *HighTech and Innovation Journal*, 2023, 4(1), 189–209. <https://doi.org/10.28991/HIJ-2023-04-01-013>
7. Sudhir M. R., Beulah M. Multigene genetic programming based prediction of concrete fracture parameters of unnotched specimens. *Civil Engineering Journal*, 2023, 9(2), 393–410. <https://doi.org/10.28991/CEJ-2023-09-02-011>
8. Van Mier J. G. M., Van Vliet M. R. A. Influence of microstructure of concrete on size/scale effects in tensile fracture. *Engineering Fracture Mechanics*, 2003, 70(16), 2281–2306. [https://doi.org/10.1016/S0013-7944\(02\)00222-9](https://doi.org/10.1016/S0013-7944(02)00222-9)
9. Gupta P. K., Singh C. A novel algorithm to model concrete based on geometrical properties of aggregate and its application. *Computers and Structures*, 2024, 292. <https://doi.org/10.1016/j.compstruc.2023.107233>
10. Thilakarathna P. S. M., Kristombu Baduge K. S., Mendis P. et al. Mesoscale modelling of concrete – A review of geometry generation, placing algorithms, constitutive relations and applications. *Engineering Fracture Mechanics*, 2020, 231. <https://doi.org/10.1016/j.engfracmech.2020.106974>
11. Naderi S., Zhang M. Meso-scale modelling of static and dynamic tensile fracture of concrete accounting for real-shape aggregates. *Cement and Concrete Composites*, 2021, 116. <https://doi.org/10.1016/j.cemconcomp.2021.104511>

- cemconcomp.2020.103889
12. Skarzyński, Nitka M., Tejchman J. Modelling of concrete fracture at aggregate level using FEM and DEM based on X-ray  $\mu$ CT images of internal structure. *Engineering Fracture Mechanics*, 2015, 147, 13–35. <https://doi.org/10.1016/j.engfracmech.2015.08.010>
  13. Gangnant A., Saliba J., La Borderie C., Morel S. Modeling of the quasibrittle fracture of concrete at meso-scale: Effect of classes of aggregates on global and local behavior. *Cement and Concrete Research*, 2016, 89, 35–44. <https://doi.org/10.1016/j.cemconres.2016.07.010>
  14. Dilbas H. Application of finite element method on recycled aggregate concrete and reinforced recycled aggregate concrete: A review. *Journal of Sustainable Construction Materials and Technologies*, 2021, 6(4), 173–191. <https://doi.org/10.14744/jscmt.2021.06>
  15. Li G., Cui S. Grain modeling and finite element simulation of damage evolution for AA5182-O aluminum alloy sheet. *Journal of Materials Research and Technology*, 2020, 9(5), 10559–10575. <https://doi.org/10.1016/j.jmrt.2020.07.089>
  16. Lakshmanan A., Yaghoobi M., Stopka K. S., Sundararaghavan V. Crystal plasticity finite element modeling of grain size and morphology effects on yield strength and extreme value fatigue response. *Journal of Materials Research and Technology*, 2022, 19, 3337–3354. <https://doi.org/10.1016/j.jmrt.2022.06.075>
  17. Palomino Ojeda J. M., Cayatopa-Calderón B. A., Quiñones Huatangari L. et al. Convolutional Neural Network for Predicting Failure Type in Concrete Cylinders During Compression Testing. *Civil Engineering Journal*, 2023, 9(9), 2105–2119. <https://doi.org/10.28991/CEJ-2023-09-09-01>
  18. Herbeaux A., Aboleinein H., Villani A. et al. Combining phase field modeling and deep learning for accurate modeling of grain structure in solidification. *Additive Manufacturing*, 2024, 81, 103994. <https://doi.org/10.1016/j.addma.2024.103994>
  19. Feng S. Z., Xu Y., Han X. et al. A phase field and deep-learning based approach for accurate prediction of structural residual useful life. *Computer Methods in Applied Mechanics and Engineering*, 2021, 383, 113885. <https://doi.org/10.1016/j.cma.2021.113885>
  20. Kozák V., Vala J. Crack growth modelling in cementitious composites using XFEM. *Procedia Structural Integrity*, 2023, 43, 47–52. <https://doi.org/10.1016/J.PROSTR.2022.12.233>
  21. Kästner M., Müller S., Ulbricht V. XFEM modelling of inelastic material behaviour and interface failure in textile-reinforced composites. *Procedia Materials Science*, 2013, 2, 43–51. <https://doi.org/10.1016/J.MSPRO.2013.02.006>
  22. Norouzi E., Li B., Erkmen R. E. Estimating equivalent elastic properties of frozen clay soils using an XFEM-based computational homogenization. *Cold Regions Science and Technology*, 2024, 226, 104292. <https://doi.org/10.1016/J.COLDREGIONS.2024.104292>
  23. Sukumar N., Srolovitz D. J. Finite element-based model for crack propagation in polycrystalline materials. *Clinics*, 2004, 23(2–3). <https://doi.org/10.1590/S1807-03022004000200014>
  24. Lagioia R., Panteghini A. On the existence of a unique class of yield and failure criteria comprising Tresca, von Mises, Drucker–Prager, Mohr–Coulomb, Galileo–Rankine, Matsuoka–Nakai and Lade–Duncan. *Proceedings of the Royal Society A: Mathematical, Physical and Engineering Sciences*, 2016, 472(2185). <https://doi.org/10.1098/RSPA.2015.0713>
  25. Podgórski J. The criterion for determining the direction of crack propagation in a random pattern composites. *Meccanica*, 2017, 52(8), 1923–1934. <https://doi.org/10.1007/s11012-016-0523-y>
  26. Khan S. M. A., Khraisheh M. K. A new criterion for mixed mode fracture initiation based on the crack tip plastic core region. *International Journal of Plasticity*, 2004, 20(1), 55–84. [https://doi.org/10.1016/S0749-6419\(03\)00011-1](https://doi.org/10.1016/S0749-6419(03)00011-1)
  27. Westergaard H. M. Bearing Pressure and Cracks. *J. Appl. Mech.*, 1939, 61, A49–A53.
  28. Wen L.-F., Tian R., Wang L.-X., Feng C. Improved XFEM for multiple crack analysis: Accurate and efficient implementations for stress intensity factors. *Computer Methods in Applied Mechanics and Engineering*, 2023, 411, 116045. <https://doi.org/10.1016/j.cma.2023.116045>
  29. Cheng H., Zhou X. An energy-based criterion of crack branching and its application on the multi-dimensional space method. *International Journal of Solids and Structures*, 2020, 182–183, 179–192. <https://doi.org/10.1016/j.ijsolstr.2019.08.019>
  30. Faramarzi L., Rezaee H. Testing the Effects of Sample and Grain Sizes on Mechanical Properties of Concrete. *Journal of Materials in Civil Engineering*, 2018, 30. [https://doi.org/10.1061/\(ASCE\)MT.1943-5533.0002249](https://doi.org/10.1061/(ASCE)MT.1943-5533.0002249)
  31. Rezaee H., Noorian-Bidgoli M. Numerical and experimental investigation of the influence of temperature and grain size on the fracture behavior of rock. *Journal of Rock Mechanics and Geotechnical Engineering*, 2024. <https://doi.org/10.1016/j.jrmge.2024.04.023>
  32. Fuller W. B., Thompson S. E. The laws of proportioning concrete. *Transactions of the American Society of Civil Engineers*, 1907, 59(2), 67–143. <https://doi.org/10.1061/TACEAT.0001979>